OPEN ACCESS Freely available online

PLoS GENETICS

The Drosophila Zinc Finger Protein Trade Embargo Is Required for Double Strand Break Formation in Meiosis

Cathleen M. Lake[1]*, Rachel J. Nielsen[1], R. Scott Hawley[1,2]

1 Stowers Institute for Medical Research, Kansas City, Missouri, United States of America, **2** Department of Molecular and Integrative Physiology, Kansas University Medical Center, Kansas City, Kansas, United States of America

Abstract

Homologous recombination in meiosis is initiated by the programmed induction of double strand breaks (DSBs). Although the Drosophila Spo11 ortholog Mei-W68 is required for the induction of DSBs during meiotic prophase, only one other protein (Mei-P22) has been shown to be required for Mei-W68 to exert this function. We show here that the chromatin-associated protein Trade Embargo (Trem), a C2H2 zinc finger protein, is required to localize Mei-P22 to discrete foci on meiotic chromosomes, and thus to promote the formation of DSBs, making Trem the earliest known function in the process of DSB formation in Drosophila oocytes. We speculate that Trem may act by either directing the binding of Mei-P22 to preferred sites of DSB formation or by altering chromatin structure in a manner that allows Mei-P22 to form foci.

Citation: Lake CM, Nielsen RJ, Hawley RS (2011) The Drosophila Zinc Finger Protein Trade Embargo Is Required for Double Strand Break Formation in Meiosis. PLoS Genet 7(2): e1002005. doi:10.1371/journal.pgen.1002005

Editor: Gregory P. Copenhaver, The University of North Carolina at Chapel Hill, United States of America

Received October 13, 2010; **Accepted** December 21, 2010; **Published** February 24, 2011

Funding: Stowers Institute for Medical Research; American Cancer Society Research Professor Award RP-05-086-06-DDC. The funders had no role in study design, data collection and analysis, decision to publish, or preparation of the manuscript.

Competing Interests: The authors have declared that no competing interests exist.

* E-mail: cml@stowers.org

Introduction

Meiosis is a specialized form of cell division that couples one round of DNA replication with two rounds of chromosome segregation, thereby reducing the number of chromosomes by half. During meiosis I, the process of homologous recombination takes place to ensure chromosomes segregate faithfully at the anaphase I transition. The initiation of homologous recombination requires the formation of meiotically induced Double Strand Breaks (DSBs). DSB formation is a highly controlled process, both in terms of position and timing, and failing to initiate DSBs or initiating them at the wrong time or in the wrong place has severe consequences in the viability of meiotic products [1]. Therefore, understanding genes whose products are required for the initiation of homologous recombination has important implications in understanding the process of chromosome segregation during meiosis.

Most organisms are thought to initiate recombination by the evolutionarily conserved topo-isomerase-like protein Spo11. DSB formation appears to be a highly conserved mechanism, as Spo11 homologs have been found in multiple species [2]. However, in addition to Spo11, in *Saccharomyces cerevisiae* at least nine other proteins (Rec102, Rec104, Ski8, Rec114, Mei4, Mer2, Mre11, Rad50 and Xrs2) have been shown to be required for DSB formation [2]. Although many of these proteins have additional roles outside of meiosis, at least four of them are meiosis-specific proteins (Mei4, Rec102, Rec104, and Rec114) [1]. However, Spo11 is the only protein that a biochemical function has been determined in that it covalently attaches to the ends of DSBs [3,4].

In *Drosophila melanogaster*, the Spo11 ortholog is known as Mei-W68, and mutants in this gene ablate DSB formation during meiosis [5,6]. In addition to Mei-W68, only one other protein, Mei-P22, is known to be required for the formation of DSBs [7]. Previous studies have shown that Mei-P22 localizes to discrete foci in early pachytene after synaptonemal complex (SC) formation, and these foci show partial overlap with the γ-His2Av foci that mark DSBs [7,8]. We will show below that the C2H2 zinc finger protein known as Trade Embargo (Trem) is required for the localization of Mei-P22 to discrete foci on meiotic chromosomes. Moreover, as is the case for loss-of-function alleles of *mei-W68* and *mei-P22*, loss-of-function alleles of *trem* either reduce or eliminate DSB formation.

Through the formation and repair of DSBs chiasmata are formed which physically link the homologs together. Chiasmata formation is sufficient to ensure that chromosomes are aligned properly on the metaphase I spindle [9,10]. Although in Drosophila females the failure to form chiasmata on one or two chromosomes can be compensated for by the function of the distributive/achiasmate system, global defects in homologous recombination cannot be fully rescued by this system [11,12]. As a result of overwhelming the distributive system, mutants that greatly reduce exchange exhibit high levels of meiotic nondisjunction [11]. This allows us to use elevated nondisjunction as an assay for failed recombination.

The gene encoding Trem, *trade embargo*, was originally identified by the recovery of a mutant ($trem^{F9}$) from a germline clone screen for new mutants that induce high levels of meiotic nondisjunction [13]. The $trem^{F9}$ mutant displayed both high levels of nondisjunction at the first meiotic division and greatly reduced levels of meiotic recombination. A combination of SNP and deficiency mapping identified *trem* as *CG4413*, a gene encoding a protein with a Zinc finger Associated Domain (ZAD) and five C2H2 zinc fingers at the carboxy-terminus.

In this study we characterize the function of Trem within the female germline. We find that Trem is chromatin-associated and enriched in early zygotene prior to complete SC formation. In

Author Summary

The ability of sexually reproducing organisms to produce viable offspring depends on their ability to faithfully execute meiosis. Meiosis is a specialized set of two cell divisions that ensures that each sperm and egg receives only one copy of each pair of chromosomes. Thus, in human females, although virtually all somatic cells carry 23 pairs of homologous chromosomes (for a total of 46 chromosomes), the egg needs to possess only one copy of each chromosome (for a total of 23). This reduction in chromosome number requires three basic steps: the pairing of homologous chromosomes, the linking of those pairs by recombination, and the separation of those pairs into two daughter cells at the first meiotic division. Unfortunately, little is known about the mechanism(s) by which the sites of recombination are chosen. Here we describe a Drosophila protein called Trem that both binds to meiotic chromosomes and defines the first known step of recombination initiation in Drosophila. Our studies of the functional anatomy of the Trem protein and the nature of the mutant defect provide important clues to the puzzle of how recombination is initiated. Such clues will help us understand how the cell controls this critical meiotic process.

females homozygous for null alleles of *trem* no meiotic DSBs are initiated and DSBs are reduced in partial loss-of-function alleles. In addition, at least one allele of *trem*, $trem^{F9}$, ablates the ability of Mei-P22 to form foci on meiotic chromosomes. That these defects in DSB formation are solely responsible for the failures in exchange and disjunction observed in *trem* mutant females is demonstrated by our ability to partially rescue the nondisjunction phenotype by inducing DSBs using X-rays.

Trem, which is expressed prior to the appearance of Mei-P22 foci, is required for the earliest known function in the initiation of DSB formation in Drosophila. We speculate that the failure of Mei-P22 to localize to discrete foci in $trem^{F9}$ results in the failure to initiate DSBs. We reason that this may be occurring by one of two mechanisms; either Trem is physically required for recruiting Mei-P22 to future DSB sites, or Trem may be altering the chromatin structure at future DSB sites, and this alteration is a prerequisite for Mei-P22 loading.

Results

Trem, a chromatin-associated protein, is enriched in region 1 of the germarium

As noted above, $trem^{F9}$ was mapped to the *CG4413* transcription unit based on a failure to complement the meiotic nondisjunction phenotype of two overlapping deficiencies that uncover *CG4413* and a *pBac*-element insertion, $trem^{f05981}$, located in the *5′* UTR of the gene (Figure 1A and 1B) [13]. In addition, sequence analysis of the original allele of *trem*, $trem^{F9}$, identified a C to T transition, corresponding to a proline to leucine (P299L) change that was not present on the parental chromosome used for EMS mutagenesis [13]. Finally, we show here that a transgene that expresses *CG4413* from a genomic promoter (*P{trem+}*) fully suppressed the meiotic nondisjunction phenotype of $trem^{F9}$ (Table 1 and Table S1A), and that a germline expression construct (*PUASp-trem*$^{+}$) was only able to rescue this phenotype when expressed with the germline driver (*P{nos-Gal4::VP16}*) (Table S1B).

We examined the localization pattern of Trem during meiotic prophase using an antibody made against a bacterially-expressed Trem protein (Materials and Methods). As shown in Figure 1C, in wild-type ovaries *trem* is expressed within the nucleus of most cells in the ovariole, including follicle cells. However, Trem is most prominent in cells in region 1 of the germarium, the stage just prior to the initiation of meiosis in region 2A (Figure 1C). We found that Trem has a thread-like staining pattern in all cells in which it is expressed, suggesting that Trem is chromatin-associated (Figure 2). Although we were unable to detect any difference in *trem* expression or localization in $trem^{F9}$ ovaries compared to wild type, we were not able to detect *trem* expression in $trem^{f05981}$ ovaries using the polyclonal antibody, suggesting that $trem^{f05981}$ is a null allele of *trem* (Figure 1C).

Loss-of-function *trem* mutants fall into two distinct classes

Unlike females homozygous for $trem^{F9}$, homozygous $trem^{f05981}$ females were semi-sterile, producing on average one progeny per female (see Table 2A). The few progeny that are produced by such females do, however, exhibit high levels of nondisjunction (17% *X* nondisjunction) that is characteristic of the $trem^{F9}$ and other fertile alleles (see below). When we analyzed the ovaries from $trem^{f05981}$ virgin females we observed that prior to stage 6 the egg chambers appeared relatively normal, showing normal DNA morphology and specification of the oocyte (Figure S1). However, by the time the females were 2 days of age almost no late stage egg chambers could be detected in $trem^{f05981}$ females. Not only was it very rare to see egg chambers developed past stage 8, the ovaries appeared very rudimentary and showed evidence of apoptosis. The reason for the arrest is unknown. However, as shown below, this arrest is exhibited in females carrying mutations that specifically affect the three internal zinc finger domains.

Both the meiotic and oogenesis progression functions of Trem are restricted to the germline

As noted above, the $trem^{f05981}$ allele results from the insertion of a *PBac{WH}* element in the *5′* UTR. We took advantage of the UAS within the *PBac{WH}* element to determine whether the meiotic phenotype and semi-sterility of $trem^{f05981}$ were a direct result of the disruption in the *trem* gene. *PBac{WH}* elements carry a UAS at one of the ends [14], and in this case the UAS was in the appropriate orientation to drive expression of the *trem* gene. Using *P{nos-Gal4::VP16}* driver, which promotes expression in the germline from the tip of the germarium throughout the mature egg [15], we were able to restore the fertility of $trem^{f05981}$ females and rescue the increased nondisjunction observed in $trem^{F9}$/$trem^{f05981}$ transheterozygotes (Table S1C). Similarly, we were able to restore fertility of $trem^{f05981}$ females with the genomic rescue construct *P{trem+}* (see Table 2A) and the progeny of this cross showed normal levels of disjunction. No fertility defect was observed in $trem^{f05981}$ males compared to wild-type males (data not shown). Thus, for both its meiotic and oogenesis functions, Trem is only required in the germline. Given that both fertility and normal disjunction can be restored when *trem* is expressed only in the germline (using the germline specific driver *P{nos-Gal4::VP16}*) and not in the surrounding follicle cells (see Figure S2 and Table S1), the function of Trem in those follicle cells remains unclear (see Figure 1C).

A structure-function analysis of *trem*

trem is predicted to encode a 439 amino acid protein with an N-terminal ZAD and 5 C2H2-type zinc finger domains at the C-terminus (Figure 3A). As shown in Figure 3, $trem^{F9}$ results from a P-L change in a conserved residue in the linker region between the

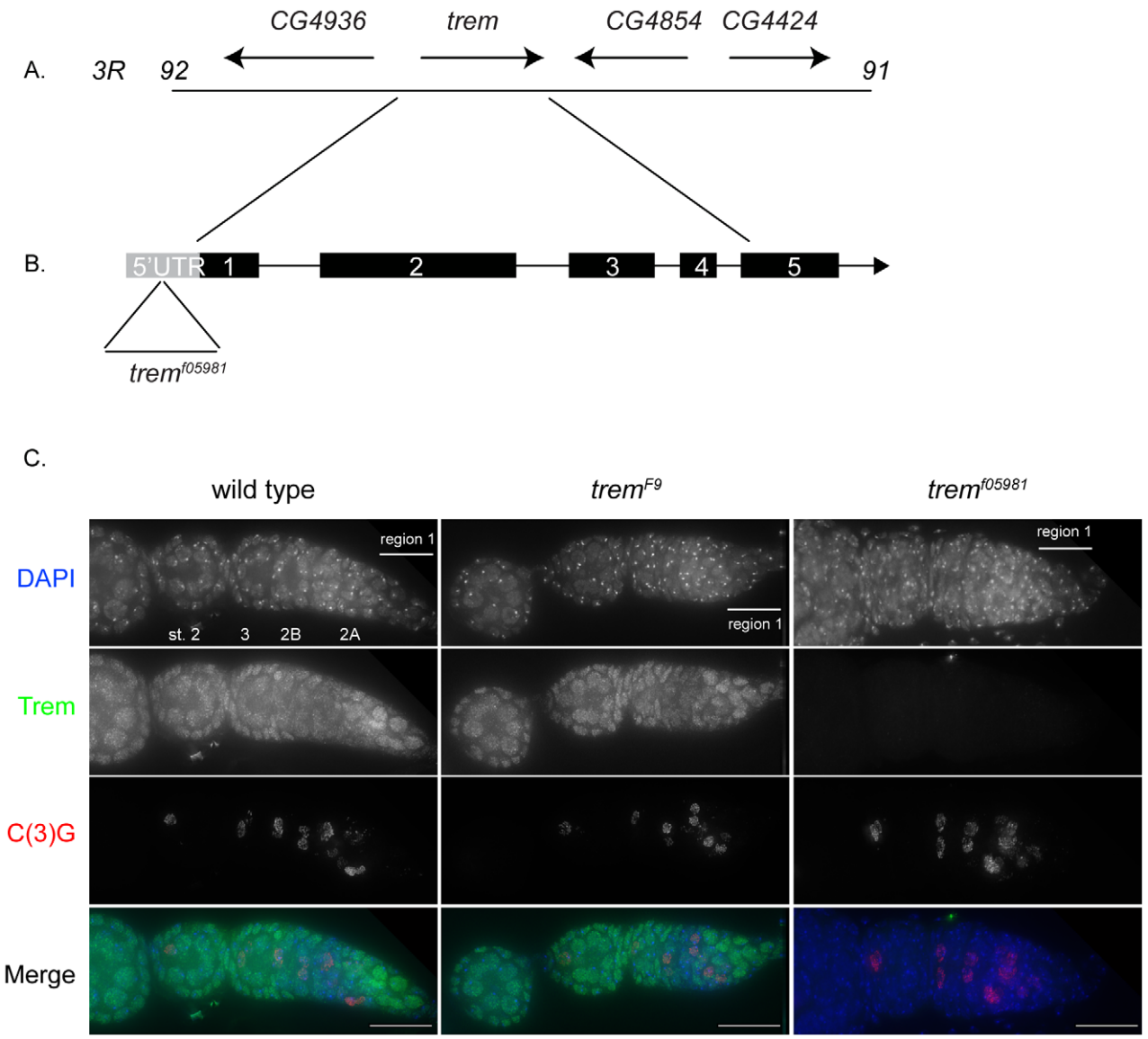

Figure 1. *trem* localization and expression. (A). Schematic diagram of the *trem* gene and its location on *3R*. *trem* is found in a cluster of 4 genes all of which are predicted to encode C2H2-type zinc finger proteins. (B) Black boxes depict the 5 exons in the *trem* gene. A *piggyBac*-element insertion used in this study, *PBac[WH]trem*^{f05981}, is located in the 5′ UTR 55 bp upstream of the start codon of *trem*. An Upstream Activation Sequence (UAS) within the *PBac{WH}*-element is oriented in the same direction as the *trem* gene. The UAS can be used to drive expression of *trem*. (C) Expression of *trem* in the germline of wild type, *trem*^{F9} and *trem*^{f05981} females. Maximum intensity projection of deconvolved Z-series through whole mount germarium stained with DAPI and antibodies to Trem and C(3)G, and the merge. Location of the developmental stages within the germarium is shown in the wild-type image. Each ovary is made up of approximately 16 ovarioles that are arranged according to developmental age [50]. In region 1, the cystoblast initiates 4 rounds of pre-meiotic divisions with incomplete cytokinesis to form a 16-cell interconnected cyst. In region 2A, meiotic prophase begins, full length SC is formed (here identified by an antibody to the major transverse filament protein C(3)G) and recombination is initiated. As the cysts move posterior, pachytene continues in region 2B (recognized by pancake shaped cysts) until it reaches region 3 where the disappearance of γ-His2Av foci indicate the repair of a DSB event. The cyst then leaves the germarium and enters the vitellarium. No observable difference could be detected in either *trem* expression or localization between wild-type and *trem*^{F9} germarium. Trem was not detected in *trem*^{f05981} ovaries, and therefore we consider it to be a null allele. In addition, no defect in SC formation (using an antibody to C(3)G) was detected in either *trem* mutant compared to wild type. Scale bar, 15 μm.
doi:10.1371/journal.pgen.1002005.g001

first and second zinc finger domain. In order to determine what role these domains play in Trem function we analyzed the phenotypes of a large number of *trem* mutants produced either by mutagenesis *in vivo* or by site-directed mutagenesis.

We first employed the Drosophila TILLING service to identify five additional missense alleles of *trem* through screening the EMS-mutagenized Chromosome *3* lines created by Zuker (Figure 3) [16]. Each of these mutants was initially analyzed by monitoring the frequency of *X* chromosome nondisjunction when heterozygous with *trem*^{f05981}. The first three alleles tested (*trem*^{4799}, *trem*^{3065} and *trem*^{0936}) caused no defect in fertility or meiotic segregation. However, both *trem*^{1272} and *trem*^{3100}, which alter amino acids located in the first zinc finger, caused nondisjunction levels similar to *trem*^{F9}/*trem*^{f05981} (Table 1). Thus all of the three missense alleles of *trem* that cause a meiotic phenotype map to the first zinc finger or linker domain between the first and second zinc finger.

Table 1. Segregation defects associated with genomic *trem* alleles.

Genotype	% *X* ND[a]	N[b]
$trem^{F9}$	33.4	425
$trem^{f05981}$/+	0.0	504
$trem^{f05981}/trem^{F9}$	25.0	1425
$trem^{f05981}/trem^{1272}$	26.4	1515
$trem^{f05981}/trem^{3100}$	26.2	648
$trem^{f05981}/trem^{0936}$	0.0	499
$trem^{f05981}/trem^{3065}$	0.3	632
$trem^{f05981}/trem^{4799}$	0.3	764

[a]Nondisjunction.
[b]Total adjusted number of progeny scored.
doi:10.1371/journal.pgen.1002005.t001

In order to determine which, if any, of the other zinc finger domains or linkers are important for the meiotic function of Trem, we generated site-specific mutations in each of the linker domains and zinc finger domains (Figure 3B). We then integrated these mutant constructs into the genome at position *25C7* using site-directed integration and tested their ability to rescue both the sterility and meiotic phenotypes in $trem^{f05981}$ homozygotes. Each of these mutants either replaced the proline in one of the linker domains to leucine (as was the case for the $trem^{F9}$ allele), or the last histidine in each of the zinc fingers to a tyrosine (as was the case for the $trem^{3100}$ allele).

As shown in Table 2A all four of the linker-domain mutants created by site-directed mutagenesis were able to rescue the fertility but not the meiotic defects observed in $trem^{f05981}$ homozygotes. All of the linker domain mutants showed a meiotic phenotype similar to that observed for $trem^{f05981}/trem^{F9}$ females (Table 1). Thus, mutations altering the proline in all four linker regions caused a strong meiotic defect without inducing semi-sterility. There was no observable difference in localization of Trem in the linker domain mutants compared to wild type suggesting that these mutations do not prevent the altered Trem protein from binding to chromatin during zygotene (data not shown).

Unlike the linker domain mutants, not all of the zinc finger domain mutants were able to rescue the semi-sterility of $trem^{f05981}$. Only the mutants in the outside fingers (1 and 5) showed an increase in progeny compared to no insert control, and both of these showed a meiotic phenotype similar to $trem^{3100}/trem^{f05981}$ females (compare Table 2B and Table 1). The site-directed mutants for zinc fingers 2, 3 and 4 showed little increase in the number of progeny produced compared to $trem^{f05981}$ females, although within the small number of progeny produced the meiotic nondisjunction phenotype was still apparent. Although the ability to invoke semi-sterility appears to be characteristic of mutations in the internal zinc fingers, the ability to increase meiotic nondisjunction appears to be a general property of mutations within all of the zinc finger domains. As was the case with the linker domain mutations none of these mutations prevented binding of the altered Trem proteins to meiotic chromosomes (see Figure S3).

We interpret these data to mean that both classes of *trem* mutations, the semi-sterile alleles that cause elevated nondisjunction and the fertile alleles that cause high levels of nondisjunction, exert their effects not by preventing the binding of Trem to the chromosomes, but rather by altering the ability of Trem to recruit or interact with other proteins. As detailed in the Discussion, the ability of C2H2 zinc finger proteins to mediate protein-protein interactions is not unprecedented [17]. We also note that although the semi-sterile alleles were restricted to the three internal zinc fingers, the meiotic nondisjunction phenotype appears to be a general property of all loss-of-function *trem* alleles.

To determine the role that the ZAD of Trem plays in the function of Trem within the germline, we created two mutants that are predicted to disrupt ZAD structure. This domain is evolutionarily conserved within arthropod genomes and the last common ancestor of arthropods and vertebrates [18,19]. It is predicted, based on studies of two Drosophila transcriptional activators (Serendipity δ and Grauzone), that these domains facilitate protein-protein interactions [20,21]. Interestingly, at least 50% of the ZAD containing proteins in Drosophila are expressed in the female germline, suggesting that proteins containing these motifs play important roles in oocyte development and/or during embryogenesis [18,19]. In general, ZADs are between 71–97 amino acids and consist of four conserved sequence blocks separated by three variable

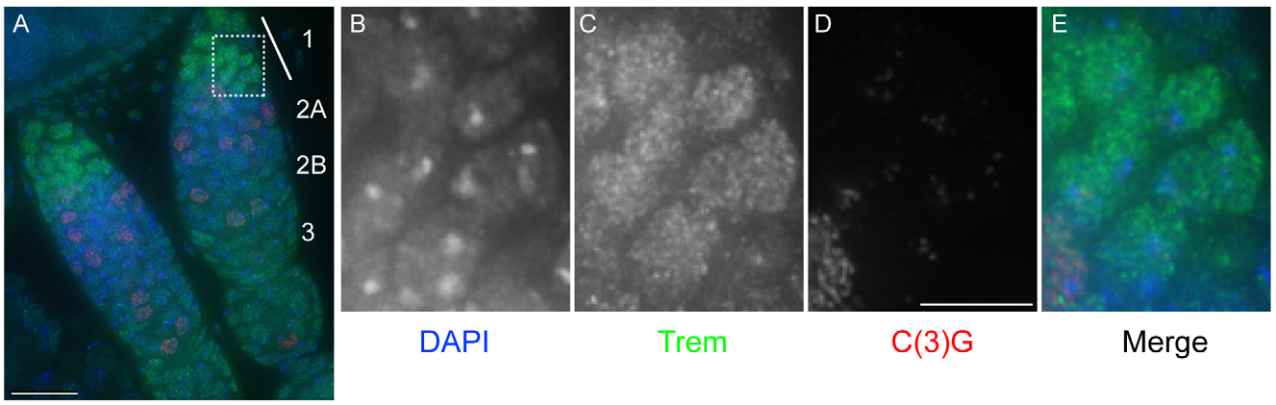

Figure 2. Trem's localization pattern suggests it is a chromatin-associated protein. (A) Maximum intensity projection of deconvolved Z-series through whole mount germarium stained with DAPI and antibodies to Trem and C(3)G. Trem appears to be expressed in most cells within the ovariole (shown is through stage 2 only), but is enriched in region 1 of the germarium. (B–E) Higher magnification of cells within the dashed box in image (A). Cells correspond to a cyst in late region 1 (zygotene), and show that Trem is chromatin associated and highly expressed in cells prior to the time full length SC is visible within the cyst in region 2A. In D, the nucleus containing full length SC corresponds to a pro-oocyte from a region 2A cyst. Little or no Trem protein was detected in the oocyte nucleus after Stage 2 (data not shown). Scale bars, 15 μm (A) and 5 μm (B–E).
doi:10.1371/journal.pgen.1002005.g002

Table 2. Segregation and fertility defects associated with *trem* mutants.

Genotype	% *X* ND[a]	N[b]	Avg. # progeny/ female
A. Defects associated with the linker domain mutants in *trem*^{f05981} homozygotes			
No insert	17	242	1
P{trem+}	0	1789	74
*P{tremP299L}**	24	1825	35
P{tremP327L}	24	767	17
P{tremP355L}	26	2071	59
P{tremP383L}	24	1606	29
B. Defects associated with the zinc finger domain mutants in *trem*^{f05981} homozygotes			
*P{tremH294Y}**	20	959	22
P{tremH322Y}	16	128	2
P{tremH350Y}	21	86	2
P{tremH378Y}	20	180	3
P{tremH406Y}	24	1264	31

[a]Nondisjunction.
[b]Total adjusted number of progeny scored.
*Denotes the same change as made within a genomic allele. *trem*^{F9} corresponds to *P{tremP299L}*, and *trem*^{3100} corresponds to *P{tremH294Y}*.
doi:10.1371/journal.pgen.1002005.t002

regions. Within two of these conserved blocks are two invariant cysteine pairs [18]. Crystallographic and biochemical studies of Grauzone have shown that the cysteines are important to coordinate zinc binding to stabilize a novel treble-clef-like structure [21].

We mutated the second cysteine in each of these conserved blocks in *trem* and expressed the mutant construct under the native promoter as we had done with all the other site-directed mutations. We were unable to detect the presence of the mutated Trem protein in a *trem*^{f05981} background by immunofluorescence for either construct (see Figure S3), which may mean either that the altered protein is no longer recognized by the polyclonal guinea pig anti-Trem antibody, or that these mutations have caused the protein to be targeted for degradation. Perhaps not surprisingly, neither mutant construct was able to rescue the sterility phenotype associated with the *trem*^{f05981} mutation (data not shown). Since the promoter region was unchanged from the other site-directed mutant constructs (all of which expressed proteins identified by the polyclonal antibody), there is no reason to speculate that the gene is not expressed. Future studies will be needed to determine what role the ZAD plays in the function of Trem during female meiosis.

trem is required for normal levels of meiotic recombination

Due to the enrichment of Trem in cells located just prior to the start of meiotic prophase and previously published data that *trem*^{F9} is defective in meiotic recombination [13]; we further analyzed the effect on recombination in *trem*^{F9} females along the *X* chromosome (Table 3). Recombination across the entire euchromatic region was reduced in a relatively uniform fashion, which is to say that *trem* does not exhibit an altered distribution in the residual crossovers that do occur. An examination of 2nd chromosome recombination in *trem*^{F9} females revealed a similar reduction to that observed on the *X* chromosome. Exchange was reduced to 11.1% of wild type across the left arm of chromosome *2*, and no changes in the exchange distribution on this chromosome were

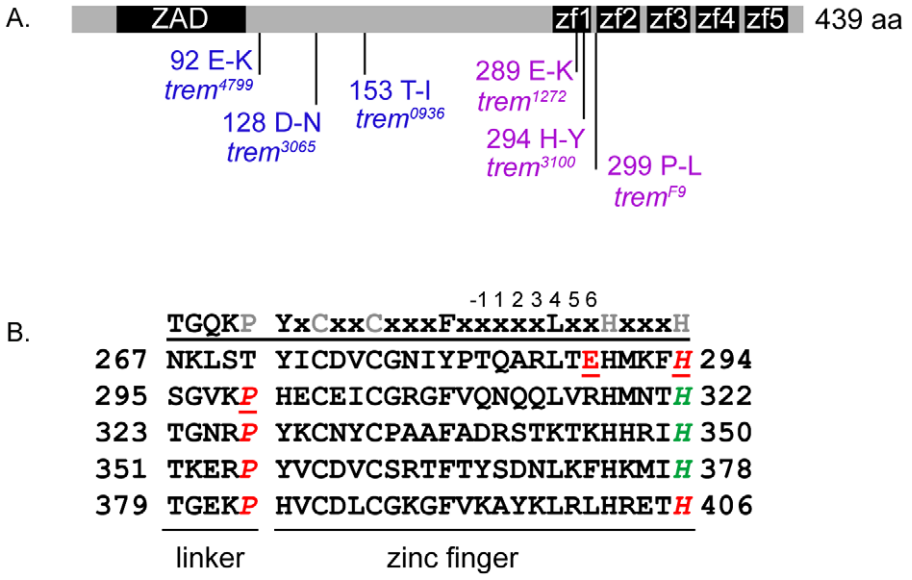

Figure 3. Genomic alleles of *trem*. (A) *trem* is predicted to encode a 439 amino acid protein that contains an N-terminal ZAD and 5 C2H2 zinc finger domains at the C-terminus (zf1–5). Schematic depiction of the location of 5 *trem* alleles obtained from TILLING *trem* and the original *trem*^{F9} allele. Meiosis defective alleles are shown in purple, and alleles that do not show a meiotic phenotype are shown in blue. (B) Sequence alignment of the 5 C2H2 zinc finger domains and linker regions of Trem. Numbers next to the sequence correspond to amino acid position. Above the Trem sequence are shown the residues typically found within C2H2-type zinc fingers and the intervals between them. The amino acid residues in grey correspond to the conserved residues within the 5 zinc fingers in Trem. The locations of the genomic *trem* alleles (*trem*^{1272}, *trem*^{3100} and *trem*^{F9}) are underlined, and italics denote the transgenic alleles. The amino acid residues in red correspond to fertile alleles, and those in green correspond to semi-sterile alleles. All linker domain mutations correspond to proline to leucine changes, and zinc finger mutations in the second conserved histidine correspond to a histidine to tyrosine change. The residues at position −1, 2, 3 and 6 are important for specifying the DNA target [26].
doi:10.1371/journal.pgen.1002005.g003

Table 3. Frequency of recombination on the *X* chromosome in genomic *trem* alleles.

Genotype	*sc-cv*	*cv-v*	*v-f*	*f-y*$^{+}$	Total Map Length (cM)	N[a]
wild type	16.15	20.02	23.17	12.50	71.84	2663
trem^{F9}	0.70	3.35	1.70	1.39	7.14	2297
trem^{F9}/*trem*^{f05981}	0.00	0.18	0.18	0.18	0.53	565
trem^{3100}/*trem*^{f05981}	0.14	0.41	0.14	0.14	0.82	733
trem^{1272}/*trem*^{f05981}	0.00	0.00	0.00	1.28	1.28	313

[a]Total number of female progeny scored.
doi:10.1371/journal.pgen.1002005.t003

observed (data not shown). The defects observed in the meiotic recombination process are not likely to be the result of defects in meiotic pairing or SC formation, as no discernable differences could be detected in pairing by FISH analysis (Figure S4) or in SC structure by immunofluorescence analysis of two SC components (data not shown and Figure 1C).

To determine if the elevated levels of nondisjunction observed in females with the missense alleles obtained from the Zuker collection also resulted from a failure to undergo wild-type levels of homologous recombination, we analyzed the frequency of recombination on the *X* chromosome in these *trem* mutants. Recombination on the *X* chromosome was reduced by more than one hundred-fold compared to control levels in *trem*^{1272}/*trem*^{f05981}, *trem*^{3100}/*trem*^{f05981} and *trem*^{F9}/*trem*^{f05981} females (Table 3). Thus, a reduction of meiotic recombination appears to be a general property of *trem* alleles.

trem is required for DSB formation

We next determined whether or not the reduced recombination observed was a result of a failure to initiate the meiotic recombination pathway. Therefore we analyzed whether *trem* mutants are able to induce meiotic DSBs.

The timing and repair of meiotically induced DSBs in Drosophila can be assayed using an antibody to the phosphorylated form of His2Av (γ-His2Av) [6,8]. As shown in Figure 4 and Table 4 we analyzed *trem* mutants for the ability to form DSBs in region 2A of the germarium using the γ-His2Av antibody. Table 4 shows that in the absence of Trem, DSBs are made at greatly reduced levels when compared to wild type for all four alleles of *trem* tested. Indeed, the reduction in DSB formation by this assay in *trem*^{f05981} females was similar to what has been reported for null alleles of the Drosophila Spo11 ortholog *mei-W68* [6] suggesting that in the absence of Trem no meiotic DSBs are formed.

To verify that the *trem* mutants were truly defective in DSB formation, and not defective in the ability to modify the DSBs through phosphorylation of His2Av, *trem*^{f05981} females were treated with X-rays to create breaks from an exogenous source. The number of DSBs created by X-ray treatment in region 2A was measured 5 hours after treatment, a time frame known to be sufficient for responding to X-ray induced breaks [8]. After 5 hours in non-treated control *trem*^{f05981} homozygotes, few if any breaks were made in pro-oocytes in region 2A of the germarium (average of 0.37 breaks without X-ray). However, in *trem*^{f05981} homozygotes treated with X-rays there were 11.3 breaks on average in region 2A (Figure 4). This level of break formation is consistent with previously published data for other mutations that affect DSB formation [8]. These results suggest that the machinery required to modify a break site if a DSB is made is not defective in

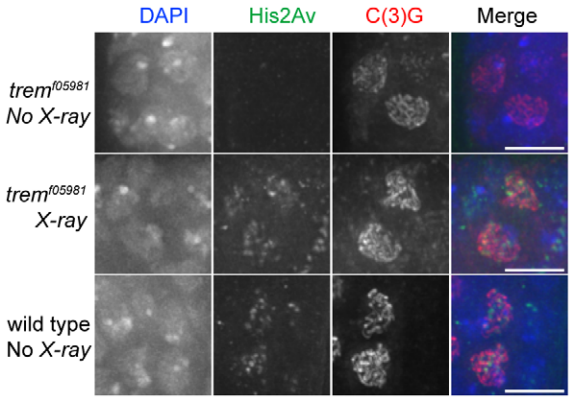

Figure 4. *trem*^{f05981} females are able to respond to breaks created by X-ray. Maximum intensity projections of deconvolved Z-series through pro-oocytes in region 2A in *trem*^{f05981} females either unexposed or exposed to 1000 Rad of X-ray stained with DAPI and antibodies to γ-His2Av and C(3)G and the merge. Unexposed wild-type pro-oocytes in region 2A are shown for comparison of qualitative differences in staining. Two adjacent cells within the cyst show the predicted thread-like pattern of SC. Average number of DSBs in region 2A in *trem*^{f05981} females is 0.4, N = 57. Average number of DSBs in *trem*^{f05981} females 5 hours after exposure to X-ray is 11.3, N = 13. Average number of DSBs in wild-type females is 12.5, N = 20 (see Table 4). Scale bar, 5 μm.
doi:10.1371/journal.pgen.1002005.g004

trem mutant oocytes, and that the defect is likely in the initiation of the DSBs.

As the formation and repair of DSBs is a dynamic process, and likely more DSBs are made than can be observed at any given time, we preformed a second assay to determine more precisely the number of DSBs created in *trem* mutant females. We analyzed the number of DSBs created in *trem*^{f05981} and *trem*^{F9} oocytes when they are simultaneously defective in the ability to repair DSBs. The two DSB repair mutants used in this study were *spnB* and *okr*. *spnB* is a Rad51-like homolog, and *okr* is the homolog of the yeast RAD54 gene, both of which are meiosis-specific genes required for DSB repair [22].

Consistent with previously published results for DSB repair defective mutants, single mutants of *spnB* and *okr* accumulate ~21 DSBs as determined by γ-His2Av foci in region 3 of the germarium (Table 5) [6]. As might have been predicted *okr*^{AA}/*okr*^{RU}; *trem*^{f05981} double mutant females were devoid of any residual DSBs in region 3 (Figure 5). Thus in the complete absence of

Table 4. Double strand break formation as measured by γ-His2Av staining.

Genotype	Average number of foci in region 2A	N[a]
+/+	12.5	20
trem^{F9}	1.7	66
trem^{f05981}	0.4	57
mei-W68^{4572}	0.4	31
trem^{f05981}/+	9.0	32
trem^{f05981}/*trem*^{3100}	1.8	35
trem^{f05981}/*trem*^{1272}	2.9	49

[a]Total number of pro-oocytes in region 2A analyzed.
doi:10.1371/journal.pgen.1002005.t004

Table 5. Double strand break formation as measured by γ-His2Av staining in DNA repair mutants.

Genotype	Average number of foci in region 3	N[a]
$spnB^{BU}$	20.9	12
$spnB^{BU}$ $trem^{F9}$	8.9	35
okr^{RU}/okr^{AA}	21.8	6
okr^{RU}/okr^{AA}; $trem^{F9}$	10.5	6
okr^{RU}/okr^{AA}; $trem^{f05981}$	0.1	12

[a]Total number of region 3 cysts analyzed.
doi:10.1371/journal.pgen.1002005.t005

Trem the failure to observe DSBs does not reflect them being more transient; but rather it appears that they simply do not occur.

However, we were surprised to find that the levels of γ-His2Av foci in $spnB^{BU}$ $trem^{F9}$ and okr^{AA}/okr^{RU}; $trem^{F9}$ double mutant females were only reduced by half in region 3 when compared to oocytes from single mutants of *spnB* and *okr* (Table 5). This might indicate that the reduction in DSB formation seen in region 2A in $trem^{F9}$ females was likely an underestimation of the number of DSBs formed; however, the reduction in DSB formation must be significant enough to account for the ~90% reduction in meiotic recombination.

Trem is required to localize Mei-P22 to discrete foci during early prophase

Prior to the time meiotic breaks are formed during prophase, the chromatin-associated Mei-P22 localizes to a number of discrete sites. Some, if not all of these sites, are thought to mark the position of future DSBs [7,8]. Mei-P22 loading occurs early in prophase in region 2A of the germarium and after SC formation [7]. There is a brief period in prophase (region 2A) in which both Mei-P22 foci and DSBs (γ-His2Av foci) are visible and often colocalize. Mei-P22 foci disappear by late region 2A prior to the time that γ-His2Av foci disappear. The disappearance of γ-His2Av foci is thought to indicate repair of a DSB event.

We used the $PUASp\text{-}mei\text{-}P22^{3XHA}$ construct (S. Mehrotra and K.S. McKim, unpublished), in combination with the germline driver *P{nos-Gal4::VP16}* to monitor the number and position of Mei-P22 foci. This construct fully rescues the meiotic nondisjunction phenotype of the DSB-deficient $mei\text{-}P22^{103}$ mutant (S. Mehrotra and K.S. McKim, unpublished, and this study Table 6). We analyzed the localization of Mei-$P22^{3XHA}$ in both $trem^{F9}$ and in *mei-P22* mutant females (Figure 6). Although we were able to detect Mei-P22 associated with chromatin in both genotypes, we did not observe any distinct Mei-P22 foci in $trem^{F9}$ (0/60 germarium analyzed). Distinct foci were present in $mei\text{-}P22^{103}$ females (50/50 germarium analyzed), as well as in the presence of wild-type Mei-P22 (data not shown). Although we would like to know whether Mei-P22 can localize to discrete foci in a *trem* null background, the only available allele is $trem^{f05981}$ which has a UAS element (see above) and therefore *trem* will be expressed in the presence of the driver used for $mei\text{-}P22^{3XHA}$ expression. Attempts to generate additional null alleles of *trem* have been unsuccessful. However, as shown in Figure 6, we were able to detect distinct foci in females that contained one copy of the $trem^{F9}$ allele and one copy of wild type *trem* that were also wild type for *mei-P22*.

In addition, we were unable to detect any increase in DSB formation (measured using an antibody to γ-His2Av) in $trem^{F9}$ females when $mei\text{-}P22^{3XHA}$ was overexpressed (data not shown). These results indicate that despite the fact that it is very common for C2H2 zinc finger proteins to be involved in transcriptional regulation [23], the failure to induce wild-type levels of DSBs is not due to a decrease in *mei-P22* expression (nor *mei-W68*, data not shown), and moreover, the absence of discrete Mei-$P22^{3XHA}$ foci indicate that Trem is the earliest known protein to function in the initiation of meiotic induced DSBs.

The meiotic phenotype of $trem^{F9}$ females, but not the semi-sterility of $trem^{f05981}$ females, can be partially rescued by X-ray treatment

Extreme decreases in fertility, as seen in $trem^{f05981}$ females, have not been reported for genes required to initiate DSBs in Drosophila. Therefore, we wanted to determine if the decrease in fertility was only a consequence of the failure to initiate DSBs,

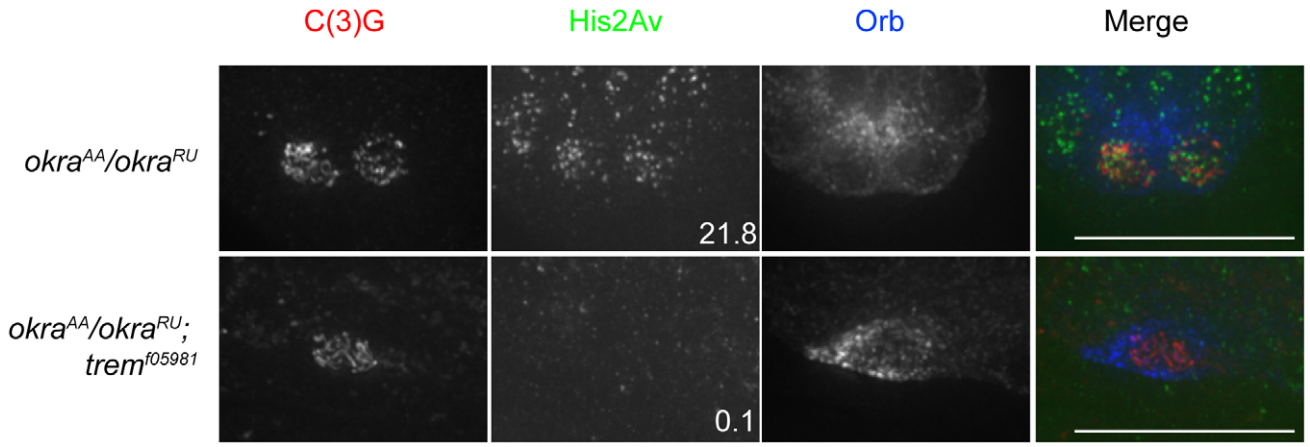

Figure 5. $trem^{f05981}$ females fail to accumulate any DSBs in region 3 in the absence of DNA repair. Using an antibody to γ-His2Av, $okra^{AA}/okra^{RU}$; $trem^{f05981}$ females fail to accumulate any DSBs in region 3 (average 0.1 compared to 21.8 for $okra^{AA}/okra^{RU}$). Images are maximum intensity projections of deconvolved Z-series through the pro-oocytes in region 3 of the germarium. Stage of oocyte was determined by position and shape of cyst within the germarium, and the pro-oocyte(s) was identified by staining with antibodies to C(3)G and Orb. $okra^{AA}/okra^{RU}$; $trem^{f05981}$ females were able to rescue the two-oocyte phenotype associated with $okra^{AA}/okra^{RU}$ indicating that the pachytene checkpoint is not activated in the absence of Trem (see Discussion). Scale bar, 15 μm.
doi:10.1371/journal.pgen.1002005.g005

Table 6. Overexpression of Mei-P22 does not rescue the nondisjunction phenotype of the *trem*^{F9} mutant.

Genotype	% *X* ND[a]	N[b]
+; PUASp-mei-P22^{3XHA}/+; mei-P22^{103}	34.4	308
+; PUASp-mei-P22^{3XHA} /+; trem^{F9}	34.6	307
P{nos-Gal4::VP16}/+; PUASp-mei-P22^{3XHA}/+; mei-P22^{103}	0.5	385
P{nos-Gal4::VP16}/ +; PUASp-mei-P22^{3XHA}/+; trem^{F9}	32.2	454

[a]Nondisjunction.
[b]Total adjusted number of progeny scored.
doi:10.1371/journal.pgen.1002005.t006

or whether Trem had a second function that rendered the females virtually sterile. We attempted to rescue the sterility defect of *trem*^{f05981} females by creating breaks with X-ray treatment. However, we saw no increase in fertility in X-ray treated *trem*^{f05981} females compared to untreated control females (data not shown). The failure to rescue fertility cannot be attributed to damage caused by X-ray, as the same dose had minimal to no effect on the fertility of wild-type females up to 6 days after treatment. The number of progeny hatched from wild-type X-ray treated females was 91% of the total number of progeny of control treated. Therefore, the defect in sterility is not attributed to the failure to form DSBs, and likely Trem has an additional later function in the germline, perhaps at the stage 8–10 transition, that is required for robust fertility.

However, if the failure to create wild-type levels of DSBs was solely causing the high levels of nondisjunction observed in *trem*^{F9} homozygotes, then we should be able to rescue these meiotic defects by inducing DSBs by X-ray. We first analyzed whether X-ray treatment could rescue the defect in prometaphase spindle formation seen in *trem*^{F9} oocytes. Oocytes from *trem*^{F9} females fail to form a single prometaphase spindle with wild-type configuration. Instead it is common to see multiple spindles, ranging from 1 to ≥4 (Figure 7). This phenotype is a direct consequence of a failure to produce the crossover events that form chiasmata which are required to maintain the integrity of the spindle during prometaphase [9,10]. Insufficient chiasmata formation resulting from failed recombination initiation will result in chromosomes failing to align and congress properly at metaphase I.

As shown in Table 7 in wild-type females 100% of the metaphase I figures appeared as a short spindle containing a mass of all chromosomes. In addition, 100% of the prometaphase figures appear as an elongated spindle with the chiasmate chromosomes in the center of the spindle and the obligate achiasmate 4th chromosomes aligned on opposite sides of the main mass [24]. However, in *trem*^{F9} females, only ~21% of the metaphase or prometaphase figures were viewed as normal and the remaining ~79% were abnormal, including figures that contained greater than 4 spindles. Upon X-ray treatment the percentage of normal to abnormal spindles shifted dramatically in *trem*^{F9}. Over 60% of the spindles appeared normal, while only ~40% were abnormal. The most apparent change can be seen looking at the fraction of oocytes with four or more separated

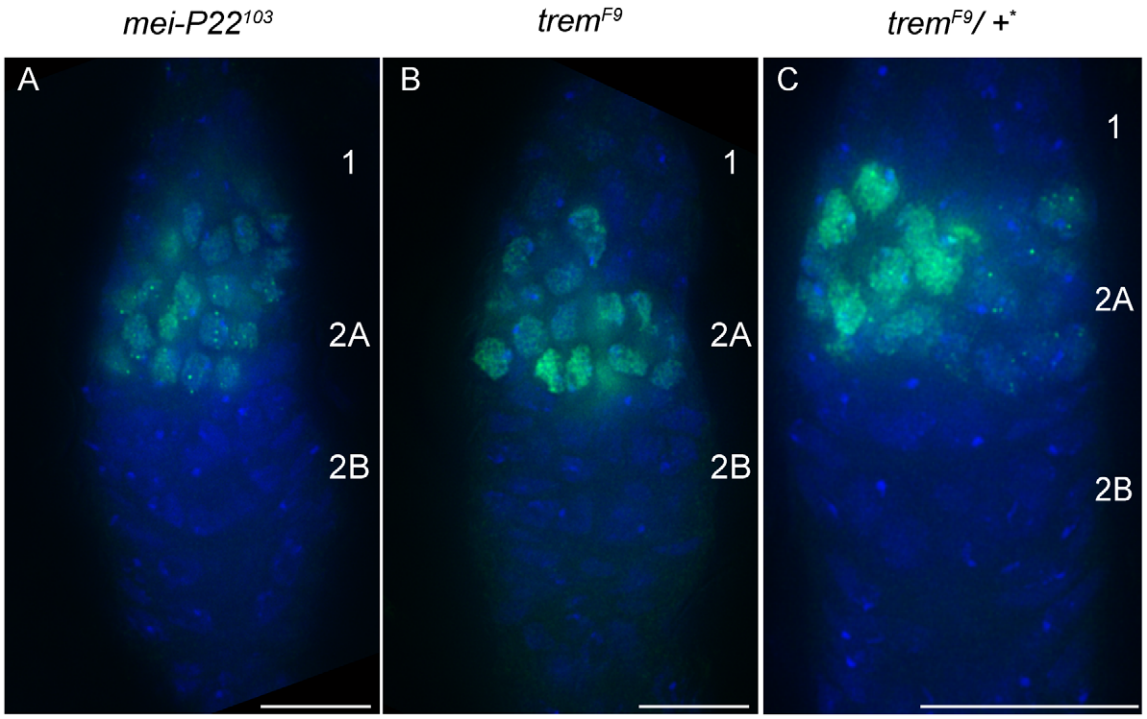

Figure 6. Mei-P22 fails to localize to discrete foci in *trem*^{F9} females. Mei-P22^{3XHA} overexpression in the germline of *trem*^{F9} females fails to localize to discrete foci in early pachytene. Maximum intensity projection of deconvolved Z-series through whole mount germarium stained with DAPI and antibodies to HA. (A) Females of the genotype *P{nos-Gal4::VP16}/+; PUASp-mei-P22*^{3XHA}*/+; mei-P22*^{103} show both chromatin-associated Mei-P22^{3XHA}, as well as its localization to discrete foci in 50/50 images. (B) Females of the genotype *P{nos-Gal4::VP16}/+; PUASp-mei-P22*^{3XHA}*/+; trem*^{F9} only show the chromatin associated localization pattern. No discrete foci were detected in 60 images analyzed. (C) Females of the genotype *P{nos-Gal4::VP16}/+; PUASp-mei-P22*^{3XHA}*/+; trem*^{F9}*/TM3, Sb* show both chromatin-associated Mei-P22^{3XHA}, as well as its localization to discrete foci in 8/8 images. (+*) chromosome is the 3rd chromosome balancer chromosome, *TM3 Sb*, and the females used were the sisters of the *P{nos-Gal4::VP16}/+; PUASp-mei-P22*^{3XHA}*/+; trem*^{F9} females in B. Germarium regions 1, 2A and 2B are shown in (A–C). Scale bars, 10 μm (A–B) and 15 μm (C).
doi:10.1371/journal.pgen.1002005.g006

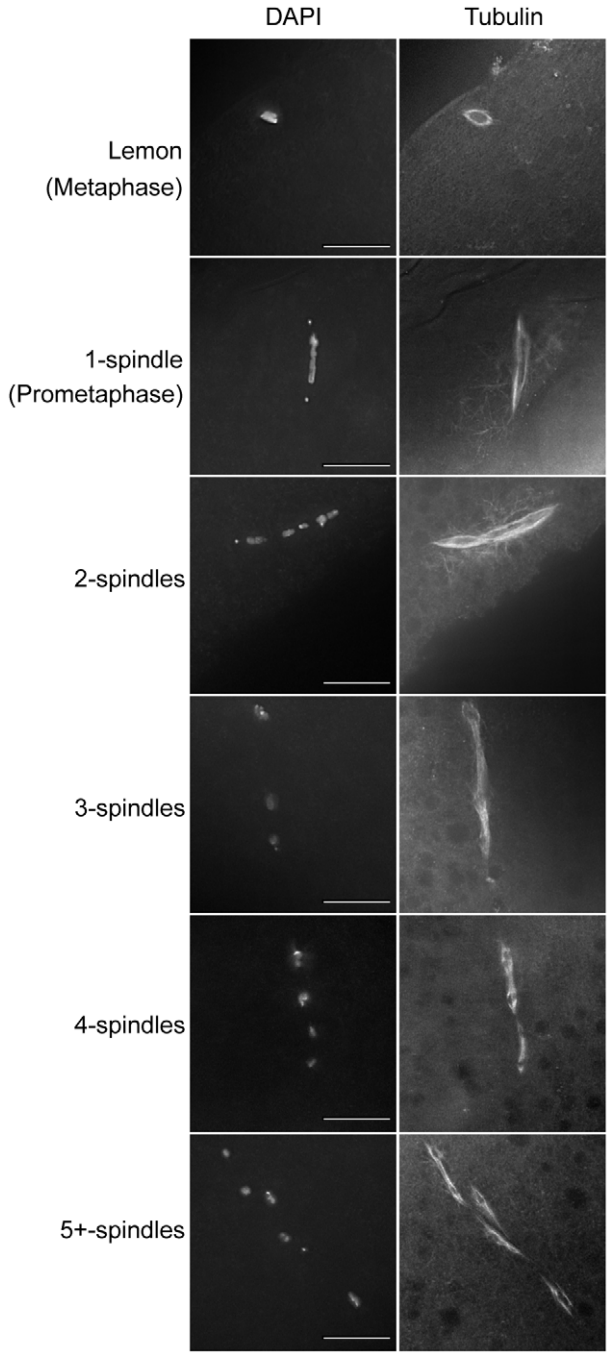

Figure 7. X-rays partially rescue prometaphase and metaphase I spindle defects associated with the *trem*^{F9} mutation. Images are maximum intensity projections of the optical sections through the tubulin staining region. Meiotic figures are stained with DAPI and tubulin, shown in gray scale. Shown are representative images from *trem*^{F9} oocytes. All images are from non-X-ray treated *trem*^{F9} females with the exception of the 3-spindle image which is from X-ray treated *trem*^{F9} females. Note that 1-spindle images in *trem*^{F9} oocytes did not necessarily have the proper DNA configuration as is seen in wild type. See Table 7 for quantification. Scale bar, 15 μm.
doi:10.1371/journal.pgen.1002005.g007

spindles which are reduced after X-ray from ~27% to ~5%. Thus, even when assayed cytologically the meiotic defect in *trem*^{F9} is a direct result of the failure to make wild-type levels of DSBs that are required to form the chiasmata necessary for ensuring proper chromosome segregation.

We also analyzed whether X-ray treatment could rescue the nondisjunction phenotype, an assay which has been shown to work for *mei-P22* mutations [7]. We compared the level of nondisjunction in *trem*^{F9} and *mei-W68*^{4572} after X-ray treatment to untreated control *trem*^{F9} and *mei-W68*^{4572} females, respectively. From a 6 day egg lay, the level of *X* nondisjunction of *trem*^{F9} females fell from 34.6% (n = 428) to 25.8% (n = 884) with X-ray treatment. There was a similar drop in *X* nondisjunction frequency seen after X-ray of *mei-W68*^{4572} females, 37.2% (n = 382) to 26% (n = 461) after treatment. Therefore the ability of X-ray to partially rescue the spindle defect and segregation defect of *trem*^{F9} females indicates that the meiotic phenotype observed is likely from a failure to initiate DSBs at wild-type levels.

trem mutants suppress the DNA damage checkpoint induced by mutants that fail to repair DSBs

The failure to repair DSBs will signal the DNA damage checkpoint leading to defects in egg polarity, sterility and karyosome formation [22,25]. These phenotypes can be suppressed by mutations that block DSB formation in the first place, such as *mei-W68* or *mei-P22* [7,25].

The failure to establish the dorsal-ventral fate of the eggshell can be analyzed by visualizing the dorsal appendages of the eggshell and comparing them to wild type (normal is two separated dorsal appendages while abnormal are fused or absent dorsal appendages). The second phenotype of checkpoint activation is the failure to form a meiotic chromosome mass known as the karyosome. Instead of spherical shaped karyosomes as is seen in wild-type stage 6 egg chambers, the karyosomes of *spnB* or *okr* oocytes are fragmented. And finally, mutants that fail to repair DSBs are sterile, or in the case of *spnB*^{BU} mutants, have significantly reduced fertility for three days after which time they become completely sterile. As shown in Table 8 and Table 9 (and Figure S5), the eggshell and karyosome defects observed in *spnB* and *okr* oocytes were almost fully suppressed in the background of *trem*^{F9}.

In addition, the *spnB*^{BU} *trem*^{F9} double mutant was fertile and this fertility persisted to at least day 10 (data not shown). As fertility of this double mutant was comparable to *trem*^{F9} females, we analyzed the frequency of recombination across the *X* chromosome and observed a meiotic recombination defect similar to *trem*^{F9} (Table 10). Although previous results have shown that in the absence of SpnB the few progeny that escape from young females show a frequency of recombination ~15% of normal and a nondisjunction rate of 12% [22], we analyzed progeny from *spnB*^{BU} *trem*^{F9} females mated for at least 10 days. Both the rate of nondisjunction (data not shown) and the frequency of recombination were more similar to *trem* mutants, and therefore we would suggest that the phenotypes observed are due to the absence of *trem* function. These results suggest that the DSBs that are created must be repaired at a later stage than normal, and the repair is done primarily through a non-crossover pathway (see Discussion).

Discussion

Trem defines the earliest known step in the initiation of recombination in Drosophila females

Until this study, only two proteins were known to be required for the initiation of programmed meiotic DSBs in Drosophila, Mei-W68 (the Spo11 ortholog) and Mei-P22. We have now identified a third protein, Trem, which is required for this process. We show that mutations in *trem* that specifically affect the zinc finger domains fail to initiate wild-type levels of DSBs, and in the

Table 7. Meiosis I spindle formation can be partially rescued in *trem*^{F9} by X-ray treatment.

	Normal		Abnormal				
Genotype	**Lemon**[a]	**1-spindle**[b]	**2-spindles**	**3-spindles**	**4-spindles**	**5+-spindles**	**N**[c]
wild type (No X-ray)	50.00	50.00					20
trem^{F9} (No X-ray)	4.17	16.67[d]	39.58	12.50	16.67	10.40	38
trem^{F9} (X-ray)	23.68	36.84[d]	21.05	13.16	2.63	2.63	48

[a]A lemon shaped spindle is the characteristic shape of a metaphase I spindle [24]. The average spindle length was 8.32 μm for wild type, 7.98 μm for *trem*^{F9} (no X-ray), and 9.18 μm for *trem*^{F9} (X-ray).
[b]The average spindle length for a prometaphase spindle was 19 μm for wild type, 18.02 μm for *trem*^{F9} (no X-ray), and 17.04 for *trem*^{F9} (X-ray).
[c]Total number of prometaphase and metaphase figures analyzed.
[d]*trem*^{F9} single spindles did not necessarily display the proper chromosome configuration.
doi:10.1371/journal.pgen.1002005.t007

complete absence of Trem no meiotic DSBs are made. In addition, we have shown that Trem is the earliest known component required for this process, in that in the presence of a mutant form of *trem*, *trem*^{F9}, Mei-P22 fails to localize into distinct foci on meiotic chromosomes. Mei-P22 is thought to mark some, if not all, of the future sites of DSBs, and therefore, we speculate that in *trem*^{F9} females the prevention of proper Mei-P22 localization results in the failure to initiate wild-type levels of DSBs.

How might Trem regulate DSB formation in Drosophila?

We can imagine two basic mechanisms by which Trem might facilitate the binding of Mei-P22 and thus the initiation of DSBs in Drosophila female meiosis. According to the first model, Trem interacts both with chromatin and one or more other adaptor proteins to facilitate the localization of Mei-P22 to discrete foci on meiotic bivalents while the second model postulates that Trem acts to modify the chromatin structure in a fashion that mediates subsequent steps in DSB formation.

The proposal that Trem interacts both with chromatin and one or more other adaptor proteins to facilitate DSB formation has its basis in previous structure-function analyses of other proteins with multiple C2H2 zinc fingers. A perhaps underappreciated role for C2H2 zinc finger proteins is the ability of multiple adjacent zinc fingers to interact with one or more proteins. A review by Brayer and Segal [17] summarizes studies of over 100 C2H2 zinc finger proteins that mediate protein-protein interactions through their zinc finger domains. Examples can be found for C2H2 proteins that interact with multiple proteins, and for C2H2 proteins that mediate both protein-DNA interactions and protein-protein interactions. These proteins can modulate both protein-DNA and protein-protein interactions not only at the same time, but also through the action of only one zinc finger. In addition, at least one example exists where the protein-protein interaction was mediated through the linker region between two adjacent zinc fingers. While neither yeast two-hybrid studies (using a germarium-derived cDNA collection) nor proteomics analysis has allowed us to identify such putative protein interactors for Trem, that effort is continuing. That said, given that Trem binding to chromatin is diffuse, Trem itself cannot be the only protein that targets the DSB-inducing machinery to sites of DSB induction.

The proposal that Trem acts to modify chromatin structure lies both in the known properties of C2H2 proteins with respect to DNA binding and a useful paradigm of a mammalian multiple C2H2 zinc finger containing protein (Prdm9). Although C2H2 zinc finger proteins can bind RNA or protein, the predominant role for C2H2 zinc finger domains is considered to be in protein-DNA recognition [23,26]. Several amino acid residues within each finger confer a specific affinity for a particular DNA sequence. The side chains of the amino acid residues at position −1, 2, 3 and 6 (see Figure 3B) make direct contact with a base and thereby determines DNA binding specificity. Therefore each finger, and combinations of multiple fingers, can lead to affinities for different DNA sequences. The linker domains that connect adjacent zinc finger domains are primarily used to help stabilize the protein-

Table 8. Rescue of eggshell defects by *trem* of the DNA repair mutant *spnB*[a].

Genotype	**% Normal**	**% Fused**	**% Absent**	**N**[b]
+/+	100			500
spnB^{BU}	38	53	8	690
trem^{F9}	97	2	1	625
spnB^{BU} *trem*^{F9}	93	3	4	664

[a]*trem*^{F9} was also able to rescue the eggshell defect associated with *okr*^{AA}/*okr*^{RU} from 24% normal to 68% normal. However, we also found that the 3rd chromosome balancer, *TM3*, was able to rescue the eggshell defect of *okr*^{AA}/*okr*^{RU} from 24% normal to 76% normal. The reason for this is unknown. Although the *TM3* balancer chromosome was able to rescue the eggshell defect; it did not rescue the sterility of the *okr* mutant.
[b]Total number of eggshells analyzed from the above genotypes. Collections were made after at least 5 days of egg laying.
doi:10.1371/journal.pgen.1002005.t008

Table 9. Rescue of karyosome defect by *trem* of the DNA repair mutants *spnB* and *okr*.

Genotype	**% Normal**	**% Abnormal**	**N**[a]
+/+	100		28
spnB^{BU}	29 (54)[b]	71	127
trem^{F9}	100 (11)[b]		35
spnB^{BU} *trem*^{F9}	98 (5)[b]	2	65
okr^{RU}/*okr*^{AA}	6	94	35
okr^{RU}/*okr*^{AA}; *trem*^{F9}	74 (21)[b]	26	43
okr^{RU}/*okr*^{AA}; *trem*^{f05981}	100 (15)[b]		75

[a]Total number of karyosomes analyzed from the above genotype from 4–7 day old mated females.
[b]Number within parentheses indicates the percentage of unfragmented but slightly abnormal spherical karyosomes that were scored as normal. Therefore, of the 100% normal karyosomes in *okr*^{RU}/*okr*^{AA}; *trem*^{f05981} females, 15% of these were slightly abnormal. Examples of this can be found in Figure S5.
doi:10.1371/journal.pgen.1002005.t009

Table 10. Frequency of crossing over on the *X* chromosome in $trem^{F9}$ females in the presence of a DNA repair mutant.

Genotype	*sc-cv*	*cv-v*	*v-f*	$f\text{-}y^{+}$	Total Map Length (cM)	N[a]
wild type	14.90	21.10	19.40	10.40	65.81	1240
$trem^{F9}$	0.47	1.63	3.26	1.40	6.74	430
$spnB^{BU}$ $trem^{F9}$	0.64	0.48	0.80	1.91	3.82	628

[a]Total number of females scored.
doi:10.1371/journal.pgen.1002005.t010

DNA interaction, but they have also been shown to function in DNA binding specificity.

Our analysis of transgenic and genomic alleles of *trem* suggest that single modifications to any of the linker domains or zinc finger domains do not ablate the ability of Trem to interact with DNA, as no difference was detected by IF with any of the alleles used in this study. Nonetheless, we can imagine that the different phenotypes produced by the two classes of *trem* mutants (semi-sterile with elevated nondisjunction, and fertile with high levels of nondisjunction) reflect the fact that these mutations disrupt the cooperative binding of the other zinc fingers which are also required for properly controlling the specificity or stability of Trem-DNA interactions.

The model that Trem might act by altering chromatin structure in a manner that is permissive for Mei-P22 binding invites a comparison with the known recombinogenic functions of another multiple zinc finger protein, Prdm9, a protein that appears to play a role in regulating the meiotic recombination pathway in mice and humans. Prdm9, which contains a zinc finger associated KRAB domain, a histone methyl transferase domain and multiple adjacent C2H2 zinc finger domains in the carboxy-terminal region of the protein, has recently been shown to localize to the hotspots of DSBs in mammalian systems [27,28,29]. Several lines of evidence suggest that Prdm9 acts at DSB hotspots through its ability to modify the chromatin and thereby targeting recombination initiation to specific sites within the genome [27,28,30,31,32,33].

Unfortunately in Drosophila, no recombination hotspots are known to exist, and therefore determining whether Trem is binding through its zinc finger domains to a specific set of conserved sequence motifs located at sites of recombination initiation is more difficult to ascertain. The comparison with Prdm9 becomes even more troubling when one considers that Trem seems to bind the entire length of chromatin rather than at a specific set of foci, such as putative hot spots. In addition, although Trem has a protein-protein interaction domain (ZAD) and multiple C2H2 zinc finger domains; no histone methyl transferase domain is found in Trem. Therefore it remains uncertain whether Trem is functioning in a similar way to Prdm9, by targeting itself to the sites of DSBs. It is also not known whether chromatin remodeling, perhaps through the action of Trem and proteins it may interact with, is as important to defining sites of recombination initiation in Drosophila as it is in yeast and mammals.

Trem is necessary for DSBs to be converted into crossovers

As noted above, we have identified a role for Trem in initiating the meiotic recombination pathway through creating programmed DSBs. However, our results suggest that Trem may also be required for processing the DSBs that are created into crossovers. We base this assertion on the observation that the DSBs that are produced in $trem^{F9}$ females are primarily repaired by a noncrossover pathway. This is not the case for hypomorphic alleles of *mei-W68* and *mei-P22*, which like $trem^{F9}$, reduce but do not ablate DSB production. In those cases the DSBs that are produced are efficiently converted into crossover events [8].

Mehrotra and McKim [8] compared the effects of weak alleles of *mei-W68* and *mei-P22* on the frequency of DSBs in region 3 of the germarium in the presence of a DSB repair mutant (as measured by the number of γ-His2Av foci) to the frequency of meiotic crossingover exhibited by these alleles in a DSB repair-proficient background. Analyzing the number of DSBs made in the DSB repair-deficient background allows for a more accurate estimate of the total number of DSBs made in each of the single mutants. This number is then divided by the total number of DSBs made in pro-oocytes in region 3 of a DSB repair-deficient mutant that is otherwise wild type for *mei-W68* and *mei-P22*, yielding the percent reduction in DSB formation for each mutant. This percent reduction in DSB formation is then compared to the degree of crossover reduction observed in single *mei-W68* and *mei-P22* mutant females relative to wild type.

For both *mei-W68* and *mei-P22* they found that the amount of crossingover, relative to wild type, was reduced substantially less than the reduction in the number of DSBs. This relationship can be expressed as a ratio of the percentage of crossingover in mutants relative to wild type divided by the percentage of DSB formation, yielding a value of ~1.5 for hypomorphs of both *mei-W68* and *mei-P22*. These observations suggest that in cases where the number of DSBs has been reduced, the fraction of DSBs processed into crossovers is in fact increased, presumably by a mechanism similar to a process called crossover homeostasis that has been well described in yeast [34].

However, we show here that in the background of the DSB repair mutant *okr*, $trem^{F9}$ accumulates 48% of the γ-His2Av foci in region 3 (see Table 5), yet $trem^{F9}$ alone shows only 9.9% crossingover compared to wild type (see Table 3). The reduction in DSB formation in $trem^{F9}$ is similar to the reduction seen in the hypomorphic alleles of *mei-W68* (at 51.4%) and *mei-P22* (at 38.3%) [8]. Therefore the ratio of crossingover to DSB formation is 0.2, far below the expected ratio of 1.5. This indicates that the fraction of DSBs created in $trem^{F9}$ females that are processed into crossover events is substantially lower than we would have expected. If $trem^{F9}$ homozygotes were comparable to *mei-W68* and *mei-P22* hypomorphs in terms of their ability to convert the DSBs that do occur into crossover events, the predicted fraction of *X* chromosomal crossingover in $trem^{F9}$ homozygotes when compared to wild-type controls would be 32%, based on a ratio of 1.5, not the observed value of 9.9%. Thus, in addition to its role in mediating the production of the initial DSB, Trem may also be required to process DSBs into crossovers, and that those DSBs that are made in $trem^{F9}$ females are repaired either by sister chromatid exchange events or gene conversions. We consider it unlikely that the DSBs are repaired to form gene conversion events, as gene conversion in Drosophila is also dependent on the normal function of Mei-P22 [35].

We can speculate that the inability of partial loss-of-function *trem* alleles to convert DSBs into crossovers is due to the failure to properly or stably localize Mei-P22 at future DSB sites. Although in $trem^{F9}$ Mei-P22 localizes to chromatin, discrete foci are never observed. It is possible that the localization of Mei-P22 into discrete foci is necessary to convert DSBs into crossovers, and in the absence of this localization, those DSBs that are formed are converted through a noncrossover pathway. The interaction between Trem and Mei-P22 may not be direct, as we observed

only a small percentage of Mei-P22^{3XHA} foci co-localized with Trem staining by IF. In the vast majority of cases Mei-P22^{3XHA} foci were observed adjacent to an area of Trem staining (Figure S6). At this time we are uncertain of the significance of the adjacency of Mei-P22 foci to Trem.

Trem may also play a role in the pachytene checkpoint

In addition to its role in DSB formation, our results suggest that Trem may also play a role in the recently elucidated pachytene checkpoint [36]. Joyce and McKim [36] showed that mutations in two classes of genes, those required for DSB repair [22] and those required for the conversion of DSBs into crossover events [37,38], resulted in activation of a pachytene checkpoint [36]. The activation of the checkpoint is associated with a delay in the chromatin remodeling process associated with DSB formation [6], as well as a delay in oocyte selection (resulting in a two-oocyte phenotype in region 3 of the germarium) [36]. For example, the delay in the selection of the oocyte exhibited by the DSB repair mutant *okr* is shown by the two C(3)G positive nuclei in the *okr* mutant in Figure 5.

Curiously, although the checkpoint seems to monitor the capacity to repair DSBs by processing them into crossover events, the checkpoint is not dependent on whether DSBs are actually formed. This is shown by the fact that null alleles of *mei-P22* and *mei-W68* do not suppress checkpoint activation in DSB repair mutants [36]. Therefore it was surprising that the *trem^{f05981}* mutant, which fails to form and accumulate any DSBs, did suppress the activation of the checkpoint in an *okr* mutant background (note the one C(3)G positive nuclei in region 3 observed in *okr*; *trem^{f05981}* double mutant in Figure 5). On the other hand, *trem^{F9}* which allows some DSBs to form did not suppress the activation of the checkpoint in an *okr* (or *spnB*) mutant background (data not shown).

To explain this data, we propose that the presence of Trem *per se*, but not its full activity, is required to activate the pachytene checkpoint in the presence of the DSB repair mutant *okr*. As the activation of the checkpoint has been purposed to result from defects in the pathway leading to crossover formation [36], it is intriguing that Trem, a protein required both to create DSBs and convert them into crossovers may be required for pachytene checkpoint activation, and that this function may be unrelated to its role in DSB formation. The mode in which Trem functions in this checkpoint will need to be further analyzed.

Materials and Methods

Drosophila strains

All Drosophila strains were maintained on standard food at 25 degrees C unless otherwise noted. Descriptions of genetic markers and chromosomes can be found at http://www.flybase.org/. Wild-type strains used in this manuscript were *yw eyFLP; FRT82B* which was the parent chromosome used to generate *trem^{F9}* [13] or Canton S. At the time of the screen we were not aware that the original *FRT P{ovo^{D1}}* chromosome had an associated lethal on the *3L* arm. To remove this lethal we generated females with the genotype *FRT82B trem^{F9}/ru h th st cu sr e ca*. Through normal recombination on these chromosomes we were able to generate the stock *ru h th st cu sr trem^{F9}*. Unless otherwise noted, *trem^{F9}* refers to *FRT82B trem^{F9}/ru h th st cu sr trem^{F9}*. Deficiency strains, *Df(3R)D1-BX12* and *Df(3R)H-B79*, where the entire *trem* protein-coding region is deleted were obtained from Bloomington Drosophila Stock Center. *P*-element insertion, *PBac[WH]trem^{f05981}* was obtained from Exelixis Collection at Harvard. *PBac[WH]-trem^{f05981}* is inserted 55 bp upstream of the start codon of *trem*. Because *PBac[WH]trem^{f05981}/Df(3R)D1-BX12* was viable, yet the *PBac[WH]trem^{f05981}* stock did not produce any *PBac[WH]trem^{f05981}* homozygotes, we speculated that the *PBac[WH]trem^{f05981}* stock contained a linked lethal. We were able to cross off a lethal from the *PBac[WH]trem^{f05981}* chromosome by allowing free recombination over a wild-type chromosome. We identified several lines that carried the *w+* from the *PBac[WH]trem^{f05981}* chromosome that produced homozygous *PBac[WH]trem^{f05981}* progeny which we refer to as *trem$^{f05981\text{-}HV}$*. We verified the presence of the *P*-element, and then analyzed the stock for fertility. As with *PBac[WH]-trem^{f05981}/Df(3R)D1-BX12* females and males, *trem$^{f05981\text{-}HV}$* homozygous females were sterile, and homozygous males were fertile. The sterility of the females could be rescued by expression of *trem* (see below). In addition, we generated the stock *FRT82B cu trem^{f05981}* by allowing free recombination in the female with the genotype *FRT82B cu sr e ca/PBac[WH]trem^{f05981}*. In this study *trem^{f05981}* refers to the genotype *FRT82B cu trem^{f05981}/trem$^{f05981\text{-}HV}$* unless noted otherwise.

Additional alleles of *trem* were obtained through TILLING of *trem* at the Fred Hutchinson Cancer Research Center (FlyTILL). Mutations were verified by sequencing. The following Zuker stocks were obtained for this study: *Z3-1272* (E289K), *Z3-3100* (H294Y), *Z3-0936* (T153I), *Z3-3065* (D128N), and *Z3-4799* (E92K). These *trem* alleles are denoted as *trem^{1272}*, *trem^{3100}*, *trem^{0936}*, *trem^{3065}* and *trem^{4799}*.

Other stocks used in this study include *y; mei-W68^{4572}* [39], *st spnB^{BU} sr e/TM6* [22], *okra^{AA} cn bw/CyO* [22], *okra^{RU} cn bw/CyO* [22], *y w; P{w+; UASp: mei-P22^{3XHA}}/ SM6* (unpublished, gift from Kim McKim), *mei-P22^{103} st/TM3, Sb* and *mei-P22^{103} th st cu e ca/ TM3, ry Sb* [7]. *mei-P22^{103}* refers to the genotype *mei-P22^{103} st/ mei-P22^{103} th st cu e ca. st spnB^{BU} sr trem^{F9}* was created for this study from females with the genotype *ru h th st cu sr trem^{F9}/ st spnB^{BU} sr e* that were allowed to recombine freely. The *spnB^{BU}* and *trem^{F9}* alleles in the stock *st spnB^{BU} sr trem^{F9}* were sequence verified.

Antibody production

The *trem* open reading frame was amplified from the *trem* cDNA RE41968 with *5′*-ggcgcgatccatatgaaaactgagtccaacg-*3′ and* 5′-*ctcgcggatcctcactctttgggggagttcat*-3′ primers and cloned into *pET-19b* (Novagen, San Diego, CA). Upon verification by sequencing, it was noticed that the original cDNA had a one base deletion at base position 1001. A cytosine was added at this position using Quik Change II XL Site-Directed Mutagenesis Kit (Stratagene, CA) to correct for the deleted base and is denoted as *pET19b-trem*. The full-length construct was verified by sequencing, and the 6×His-tagged Trem protein was expressed in *E. coli* BL21 cells. The bacterially expressed protein was purified using ProBond Nickel-Chelating Resin (Invitrogen, CA). Polyclonal antibody production in guinea pigs using purified 6×His-Trem as antigen was performed by Cocalico Biologicals (Reamstown, PA). Pre-immune sera from the immunized guinea pigs did not stain Drosophila ovaries (data not shown). Anti-Trem guinea pig antibody was affinity purified by passing serum over a Sulfo-linked Trem protein column (Thermo Fisher Scientific, IL).

Generation of transgenes

The genomic rescue construct was constructed by cloning a 2.7 kb *Pst1* fragment from Bac clone RP98-33G16 (BacPac Resources). This fragment which contains the entire gene region of *trem* plus 720 bases *5′* to *trem* (the *5′* UTR and 83 bases of coding region of *CG4936*) and 324 bases *3′* to the *trem* gene was cloned into *pCasPeR4-attB* (gift from Perrimon lab) [40] that was previously digested with *Pst*I. *pCasPeR4-attB-trem*, denoted as

p{trem^{+}*}* was introduced into Drosophila by targeted integration using the *attP-40* line (Genetic Services, MA).

The germline expression construct was generated by amplifying the full length *trem cDNA* sequence with primers *5′*-cttacgggccg-catgaaaactgagtcc-*3′ and 5′-gcggtctagatcactctttggggag-3′* from *pET19b-trem* (above). The PCR product was digested with *Kpn*I and *Not*I and cloned into the *pUASp* vector (gift from Dr. Pernille Rørth) [15] digested with the same enzymes. Sequence was verified and *p{UASp-trem*$^{+}$*}* was introduced into Drosophila by standard P element mediated transformation protocols. Germline expression was achieved by expressing the *P{UASp-trem*$^{+}$*}* construct under the control of the *nos-Gal4::VP16* driver [15]. Virgin females of the genotype *P{nos-Gal4::VP16; FRT82B trem*^{F9}*/TM3 or yw; FRT82B trem*^{F9}*/TM3* were crossed to *P{UASp-trem*$^{+}$*}; ru h th st cu sr trem*^{F9}*/ TM3* males. Virgin females of the appropriate genotype were crossed individually to tester males and the frequency of *X* nondisjunction was determined (see below).

Generation and analysis of site-directed mutants

Mutations in *trem* were made using the Quik Change II XL Site-Directed Mutagenesis Kit (Stratagene, CA). The 2.7 kb *Pst*I fragment from Bac clone RP98-33G16 was cloned into *pBS-KS+* (Clontech, CA), denoted as *pBS-trem*, and used to generate site directed mutants. A 2.5 kb *Age*I-*Nae*I fragment from *pBS-trem* containing the engineered mutation was then cloned into *pCasPeR4*-attB digested with the same enzymes. The entire *trem* gene region was sequenced and then introduced into Drosophila by targeted integration using the *attP-40* line.

One transformant for each mutation was analyzed for the ability to rescue the sterility of *trem*^{f05981}, as well as for expression of *trem* by immunofluorescence using anti-Trem antibody (above). For the constructs that failed to rescue sterility of *trem*^{f05981}, but were expressed, a second transformant was tested. When compared to wild type no observable defects could be detected in the localization pattern of any of the site directed mutants tested in this study (see Figure S3 for examples).

Nondisjunction and recombination assays

To measure the frequency of meiotic nondisjunction of the *X* chromosome, virgin females of the listed genotype were crossed individually to *y sc cv v f y*$^{+}$*/ B[S]Y* males [41,42].

The frequency of recombination on the *X* chromosome was measured by crossing *y w/ y sc cv v f y*$^{+}$; + (wild type), *y w/ y sc cv v f y*$^{+}$*; trem*^{F9}, *y w/ y sc cv v f y*$^{+}$*; spnB*^{BU} *trem*^{F9}, *y w/ y sc cv v f y*$^{+}$*; trem*^{f05981}*/ trem*^{F9}, *y w/ y sc cv v f y*$^{+}$*; trem*^{f05981}*/ trem*^{3100}, or *y w/ y sc cv v f y*$^{+}$*; trem*^{f05981}*/ trem*^{1272} single female virgins to *y sc cv v f y*$^{+}$*/ B[S]Y* males. Only female progeny resulting from the above cross were analyzed for the markers *y sc cv v f* and *y*$^{+}$ [43,44].

Sequencing

Genomic DNA was prepared from a single male fly by standard protocol [45]. *trem* gene primers used for sequencing include: *5′*-gcgtctcaccgagcacatga-*3′*, *5′-agctgccttcgccgatcgat-3′*; *5′*-gtcgttcataa-cgtgcattcaccg-*3′*,*5′-tgactggcgtagtcctcccacgac-3′*; *5′*-ctcctctgtggcaacatct-g-*3′*, *5′-cgcactcgtgtggtttaacaccag-*3′ and *5′*-gttcgatgtgcacgatcccacg-*3′*.

Cytology

Approximately 30–40 females, which had eclosed 2–3 days previously, were mated to 10–15 males and fed on yeast for 2–3 days prior to egg chamber dissection. These females were anesthetized and the abdomens were ruptured one by one with forceps. For early egg chambers, oocytes were fixed using previously published methods [44] with minor exceptions. Ovaries were dissected in PBS and immediately fixed for 20 min in 200 µL of PBS containing 2% formaldehyde (Ted Pella) and 0.5% Nonidet P-40 plus 600 µL heptane. Fixed ovaries were washed three times for 15 min each in PBS containing 0.1% Tween-20 (PBS-Tween-20). Ovarioles were teased apart with forceps and blocked for 1 h in PBS-Tween-20 and 1% Bovine Serum Albumin (Calbiochem) at room temperature. Primary antibody was incubated overnight at 4 C, washed as before, and secondary antibodies were applied for 4 h at room temperature. 10 min prior to washing a final concentration of 1.0 ug/mL 4′6-diamididino-2-phenylindole (DAPI) was added. Ovarioles were washed as before and mounted in ProLong Gold (Invitrogen). Late stage oocytes were fixed as previously described [46]. Whole ovaries were dissected in 1× Robb's media (55 mM sodium acetate, 8 mM potassium acetate, 20 mM sucrose, 2 mM glucose, 0.44 mM MgCl2, 0.1 mM CaCl2 and 20 mM HEPES, pH 7.4) containing 1% BSA and individually ovarioles were teased apart with forceps. Ovaries were fixed in solution containing 1× Fix Buffer (100 mM potassium cacodylate, 100 mM sucrose, 40 mM sodium acetate and 10 mM EGTA) and 8% Formaldehyde (Ted Pella) for 5 min. Ovaries were washed in PBS-0.1% Triton (PBS-Triton) 3 times for 15 min each, vitelline membrane was removed by rolling ovaries between frosted slides, and then ovaries were blocked 1 hr in PBS-Triton containing 5% Normal Goat Serum. Antibody labeling was done as described above except washes were done in PBS-Triton.

Microscopy was conducted using a DeltaVision microscopy system (Applied Precision, Issaquah, WA) equipped with an Olympus 1×70 inverted microscope and high-resolution CCD camera. The images were deconvolved using the SoftWoRx v.25 software (Applied Precision) and projected with multiple stacks.

Mouse anti-Orb antibodies (4H8 and 6H4) obtained from Iowa Hybridoma Bank [47] were used together at a 1:60 dilution. Guinea pig anti-Trem was used at 1:2500. Mouse anti-C(3)G antibody 1A8-1G2 [48] was used at a dilution of 1:500. Guinea pig C(3)G antibody was used at a dilution of 1:500 [44]. Rabbit anti-His2Av [8] was used at 1:500. Rabbit anti-Vasa [49] was used at 1:2000. Rat anti-HA clone 3F10 was used at 1:100 (Roche). Rat anti-tubulin alpha antibody (AbD Serotec, NC) was used at a dilution of 1:250. Secondary goat anti-mouse, rabbit or rat Alexa-488, Alexa-555 or Alexa-647 conjugated antibodies (Molecular Probes) were used at 1:500.

X-ray treatment

For analysis of DSBs created by X-ray, 2 day old virgin *trem*^{f05981} females were exposed to 1000 rad of X-ray at a dose of 112 rad/min and introduced to wild-type males. Ovaries from treated or non-treated control females were collected and fixed 5 hours after X-ray treatment. Immunofluorescence analysis (see above) was used to detect DSBs with the His2Av antibody [8]. For analysis of rescue of nondisjunction by X-ray, 2 day old virgin females of the appropriate genotype were exposed to X-ray as above. Females were mated individually to *y sc cv v f y*$^{+}$*/ B[S]Y* males [41,42] and progeny were scored (see above). For rescue of meiosis I spindle defects, 1 to 2 day old virgin *yw* or *yw; trem*^{F9} females were collected. Half of the *yw; trem*^{F9} females (approximately 120) were exposed to 4000 rad of X-ray at a dose of 112 rad/min, and all virgins were mated for 5 days to wild-type males. Ovaries were collected and prepared as described above.

Supporting Information

Figure S1 *trem*^{f05981} ovaries fail to develop past stage 8/9 of oogenesis. Egg chamber development in virgin (0–24 hours) and 2-day old mated females was analyzed in wild type and *trem*^{f05981}. (A–

B) In virgin ovaries, progression of egg chamber formation was analyzed by staining the ovaries with DAPI (blue) to identify nurse cell morphology for staging, and antibodies to Vasa (red) and Orb (green) to aid in identification of egg chamber staging. Orb begins to accumulate in early 8–16 cell cysts within the germarium, and Orb protein is clearly visible in whole mount ovaries within the oocyte cytoplasm at stage 6 (located at the posterior end of the egg chamber). Arrows denote similarly staged (stage 6) egg chambers in wild type and $trem^{f05981}$. The asterisk denotes the most mature egg chamber in wild type. No egg chambers of this stage were detected in $trem^{f05981}$virgin ovaries. No observable defects were detected prior to stage 6 in $trem^{f05981}$ females by this analysis. (C–D) Two day old mated females of the same genotype were analyzed for progression of egg chamber formation by staining with DAPI only. In wild-type ovaries it was very common to see late stage egg chambers, stage 9/10 denoted by arrow (note the migration of border cells which separate the germline nurse cells from the oocyte), and stage 13/14 denoted by asterisk. However, in $trem^{f05981}$very few egg chambers developed past stage 8 rendering the females semi-sterile (note the rudimentary size of the ovary). In very rare cases a late stage egg chamber could be detected in $trem^{f05981}$ ovaries. In addition, it was common to see egg chambers that appeared to be apoptotic based on irregular and fragmented nurse cell DNA at the base of the ovary (arrowhead). This arrest phenotype is due to the absence of Trem, as germline expression of *trem* in $trem^{f05981}$ background rescues fertility. Scale bar, 90 μm.
(TIF)

Figure S2 Expression of Trem from the UAS within the *PBac{WH}* element in the *5′* UTR of *trem* ($trem^{f05981}$). The germline specific promoter *P{nos-Gal4::VP16}* can drive expression of *trem* from this element. Image is a maximum intensity projection of a deconvolved Z-series through *P{nos-Gal4::VP16}/+;* $trem^{f05981}$ germarium stained with DAPI (blue) and antibodies to Trem (green) and C(3)G (red), and the merge. Expression pattern of *trem* was similar to nanos expression throughout the ovariole (only showing germarium in this figure) and localization pattern within the cell is similar to wild-type expression. Germarium regions are shown in the merge image. Scale bar, 10 μm.
(TIF)

Figure S3 *trem* localization and expression in the site-directed mutants. Expression of genomic *trem* constructs in the background of $trem^{f05981}$using an antibody against Trem (green) and DAPI (blue). (A) *P{trem+)*, the wild-type *trem* gene which rescues both fertility of $trem^{f05981}$ and the nondisjunction phenotype of *trem* mutants (B) *P{tremH294Y}*, a construct that partially rescues fertility of $trem^{f05981}$ females, (C) *P{tremH322Y}*, a construct that fails to rescue fertility of $trem^{f05981}$ females and (D) *P{tremZAD2}*, a construct that mutates the second cysteine of the second invariant cysteine pair from a C–G. We failed to detect the mutated Trem protein using the anti-Trem antibody. All images are maximum intensity projections of deconvolved Z-series through the germarium and are oriented with region 1 of the germarium to the left. Scale bar, 15 μm.
(TIF)

Figure S4 Euchromatic pairing is normal in *trem* mutants. Overlapping Bac clones from each cytolocation were fluorescently labeled using ARES Alex Fluor DNA labeling kit (Invitrogen). *trem* mutants display normal meiotic pairing at 2 euchromatic loci on the *X* chromosome (*7A–E* and *14A–B*). In addition, $trem^{F9}$ displays normal meiotic pairing at euchromatic locus *25* on the 2^{nd} chromosome. Region 2A pro-oocyte nuclei were identified by simultaneously immuno-staining with an antibody to C(3)G. The number of nuclei analyzed is shown within each bar. Nuclei containing a single focus or foci separated by 0.7 μm or less are defined as paired. To put this level of euchromatic pairing into perspective, mutants that do not form normal SC, display a 55–65% reduction in pairing [51].
(TIF)

Figure S5 $trem^{f05981}$ can rescue the karyosome defect associated with *okr* mutants. Representative images from stage 8 egg chambers from (A) $okra^{AA}/okra^{RU}$ and (B) $okra^{AA}/okra^{RU}$; $trem^{f05981}$ stained with DAPI. All images are maximum intensity projections of deconvolved Z-series through the karyosome. The karyosome structure is fragmented in $okra^{AA}/okra^{RU}$. (B) Most (85%) of the karyosomes display a normal structure, however, 15% are slightly abnormal (B′) in appearance. The reason for this is unclear. Scale bar, 10 μm.
(TIF)

Figure S6 Mei-$P22^{3XHA}$ foci tend to localize adjacent to regions of Trem. Region 2A nuclei from *P{nos-Gal4::VP16}/+; PUASp-mei-*$P22^{3XHA}$*/+; D/+* females were stained with DAPI (D) (blue) and antibodies to HA (H) (green) and Trem (T) (red) and the merge (M). Images are from a single 0.2 μm deconvolved Z-section. One Mei-$P22^{3XHA}$ foci from each nucleus (identified by the dashed box in the merge) is shown to the right. The Z-section selected for each image is from the brightest signal from the foci in the dashed box. The percent of Mei-$P22^{3XHA}$ foci in each category is shown at the right. (A) Two examples of Mei-$P22^{3XHA}$ foci located adjacent to a region of Trem. Of the 43 Mei-$P22^{3XHA}$ foci analyzed from 5 germarium 86% of the foci were found adjacent to a region of Trem. (B) Mei-$P22^{3XHA}$ foci co-localized with a bright region of Trem. (C) Mei-$P22^{3XHA}$ foci not located near Trem. Scale bar, 1 μm.
(TIF)

Table S1 Rescue of disjunction and sterility defects associated with *trem* mutants.
(DOC)

Acknowledgments

We would like to thank Kim McKim for reagents and stocks. We would like to acknowledge the work done by the SIMR Molecular Biology department for generating the site directed mutants and Genetic Services for generating the transformants used in this study. Bloomington, Fred Hutchinson Cancer Research, and the Schüpbach lab provided us with Drosophila stocks.

Author Contributions

Conceived and designed the experiments: CML RJN RSH. Performed the experiments: CML RJN. Analyzed the data: CML RJN RSH. Contributed reagents/materials/analysis tools: CML RJN. Wrote the paper: CML RJN RSH.

References

1. Murakami H, Keeney S (2008) Regulating the formation of DNA double-strand breaks in meiosis. Genes & Development 22: 286–292.
2. Keeney S (2001) Mechanism and control of meiotic recombination initiation. Current Topics in Developmental Biology: Academic Press. pp 1–53.

3. Bergerat A, de Massy B, Gadelle D, Varoutas P-C, Nicolas A, et al. (1997) An atypical topoisomerase II from archaea with implications for meiotic recombination. Nature 386: 414–417.
4. Keeney S, Giroux CN, Kleckner N (1997) Meiosis-specific DNA double-strand breaks are catalyzed by Spo11, a member of a widely conserved protein family. Cell 88: 375–384.
5. McKim KS, Hayashi-Hagihara A (1998) mei-W68 in Drosophila melanogaster encodes a Spo11 homolog: evidence that the mechanism for initiating meiotic recombination is conserved. Genes Dev 12: 2932–2942.
6. Jang JK, Sherizen DE, Bhagat R, Manheim EA, McKim KS (2003) Relationship of DNA double-strand breaks to synapsis in Drosophila. J Cell Sci 116: 3069–3077.
7. Liu H, Jang JK, Kato N, McKim KS (2002) mei-P22 Encodes a Chromosome-Associated Protein Required for the Initiation of Meiotic Recombination in Drosophila melanogaster. Genetics 162: 245–258.
8. Mehrotra S, McKim KS (2006) Temporal Analysis of Meiotic DNA Double-Strand Break Formation and Repair in *Drosophila* Females. PLoS Genet 2: e200. doi:10.1371/journal.pgen.0020200.
9. McKim KS, Jang JK, Theurkauf WE, Hawley RS (1993) Mechanical basis of meiotic metaphase arrest. Nature 362: 364–366.
10. Jang JK, Messina L, Erdman MB, Arbel T, Hawley RS (1995) Induction of metaphase arrest in Drosophila oocytes by chiasma-based kinetochore tension. Science 268: 1917–1919.
11. Baker BS, Hall JC (1976) Meiotic mutants: genetic control of meiotic recombination and chromosome segregation. In: Ashburner M, Novitski E, eds. The Genetics and Biology of *Drosophila* Vol 1a. New YorkNY: Academic Press. pp 351–434.
12. Hawley RS, McKim KS, Arbel T (1993) Meiotic segregation in Drosophila melanogaster females: molecules, mechanisms, and myths. Annu Rev Genet. pp 281–317.
13. Page SL, Nielsen R, Teeter K, Lake CM, Ong S, et al. (2007) A Germline Clone Screen for Meiotic Mutants in *Drosophila melanogaster*. FLY 1: 172–181.
14. Thibault ST, Singer MA, Miyazaki WY, Milash B, Dompe NA, et al. (2004) A complementary transposon tool kit for Drosophila melanogaster using P and piggyBac. Nat Genet 36: 283–287.
15. Rorth P (1998) Gal4 in the Drosophila female germline. Mech Dev 78: 113–118.
16. Koundakjian EJ, Cowan DM, Hardy RW, Becker AH (2004) The Zuker Collection: A Resource for the Analysis of Autosomal Gene Function in Drosophila melanogaster. Genetics 167: 203–206.
17. Brayer K, Kulshreshtha S, Segal D (2008) The Protein-Binding Potential of C2H2 Zinc Finger Domains. Cell Biochemistry and Biophysics 51: 9–19.
18. Chung H-R, Schäfer U, Herbert J, Böhm S (2002) Genomic expansion and clustering of ZAD-containing C2H2 zinc-finger genes in Drosophila. EMBO reports 3: 1158–1162.
19. Chung H-R, Lohr U, Jackle H (2007) Lineage-specific expansion of the Zinc Finger Associated Domain ZAD. Molecular Biology and Evolution 24: 1934–1943.
20. Payre F, Buono P, Vanzo N, Vincent A (1997) Two types of zinc fingers are required for dimerization of the serendipity delta transcriptional activator. Mol Cell Biol 17: 3137–3145.
21. Jauch R, Bourenkov GP, Chung H-R, Urlaub H, Reidt U, et al. (2003) The Zinc Finger-Associated Domain of the Drosophila Transcription Factor Grauzone Is a Novel Zinc-Coordinating Protein-Protein Interaction Module. Structure (London, England : 1993) 11: 1393–1402.
22. Ghabrial A, Ray RP, Schupbach T (1998) okra and spindle-B encode components of the RAD52 DNA repair pathway and affect meiosis and patterning in Drosophila oogenesis. Genes & Development 12: 2711–2723.
23. Pabo CO, Peisach E, Grant RA (2001) Design and selection of novel Cys2His2 zinc finger proteins. Annual Review of Biochemistry 70: 313–340.
24. Gilliland WD, Hughes SF, Vietti DR, Hawley RS (2009) Congression of achiasmate chromosomes to the metaphase plate in Drosophila melanogaster oocytes. Dev Biol 325: 122–128.
25. Ghabrial A, Schupbach T (1999) Activation of a meiotic checkpoint regulates translation of Gurken during Drosophila oogenesis. Nat Cell Biol 1: 354–357.
26. Iuchi S (2001) Three classes of C2H2 zinc finger proteins. Cellular and Molecular Life Sciences 58: 625–635.
27. Baudat F, Buard J, Grey C, Fledel-Alon A, Ober C, et al. (2010) PRDM9 Is a Major Determinant of Meiotic Recombination Hotspots in Humans and Mice. Science 327: 836–840.
28. Myers S, Bowden R, Tumian A, Bontrop RE, Freeman C, et al. (2010) Drive Against Hotspot Motifs in Primates Implicates the PRDM9 Gene in Meiotic Recombination. Science 327: 876–879.
29. Parvanov ED, Petkov PM, Paigen K (2010) Prdm9 Controls Activation of Mammalian Recombination Hotspots. Science 327: 835.
30. Myers S, Freeman C, Auton A, Donnelly P, McVean G (2008) A common sequence motif associated with recombination hot spots and genome instability in humans. Nat Genet 40: 1124–1129.
31. Buard J, Barthes P, Grey C, de Massy B (2009) Distinct histone modifications define initiation and repair of meiotic recombination in the mouse. EMBO J 28: 2616–2624.
32. Borde V, Robine N, Lin W, Bonfils S, Geli V, et al. (2009) Histone H3 lysine 4 trimethylation marks meiotic recombination initiation sites. EMBO J 28: 99–111.
33. Berg IL, Neumann R, Lam K-WG, Sarbajna S, Odenthal-Hesse L, et al. (2010) PRDM9 variation strongly influences recombination hot-spot activity and meiotic instability in humans. Nat Genet 42: 859–863.
34. Martini E, Diaz RL, Hunter N, Keeney S (2006) Crossover Homeostasis in Yeast Meiosis. Cell 126: 285–295.
35. McKim KS, Green-Marroquin BL, Sekelsky JJ, Chin G, Steinberg C, et al. (1998) Meiotic synapsis in the absence of recombination. Science 279: 876–878.
36. Joyce EF, McKim KS (2009) Drosophila PCH2 Is Required for a Pachytene Checkpoint That Monitors Double-Strand-Break-Independent Events Leading to Meiotic Crossover Formation. Genetics 181: 39–51.
37. Baker BS, Hall JC (1976) Meiotic Mutants: Genetic control of of meiotic recombination and chromosome segregation. In: Ashburner M, Novitski E, eds. The Genetics and Biology of Drosophila. London: Academic Press. pp 352–434.
38. Carpenter AT, Sandler L (1974) On recombination-defective meiotic mutants in Drosophila melanogaster. Genetics 76: 453–475.
39. Bhagat R, Manheim EA, Sherizen DE, McKim KS (2004) Studies on crossover-specific mutants and the distribution of crossing over in *Drosophila* females. Cytogenetic and Genome Research 107: 160–171.
40. Markstein M, Pitsouli C, Villalta C, Celniker SE, Perrimon N (2008) Exploiting position effects and the gypsy retrovirus insulator to engineer precisely expressed transgenes. Nat Genet 40: 476–483.
41. Zimmering S (1976) Genetic and cytogenetic aspects of altered segregation phenomena in *Drosophila*. In: Ashburner M, Novitski E, eds. The Genetics and Biology of *Drosophila* Vol 1a. New York: Academic Press. pp 569–613.
42. Matsubayashi H, Yamamoto M-T (2003) REC, a new member of the MCM-related protein family, is required for meiotic recombination in Drosophila. Genes & Genetic Systems 78: 363–371.
43. Page SL, McKim KS, Deneen B, Van Hook TL, Hawley RS (2000) Genetic studies of mei-P26 reveal a link between the processes that control germ cell proliferation in both sexes and those that control meiotic exchange in Drosophila. Genetics 155: 1757–1772.
44. Page SL, Hawley RS (2001) c(3)G encodes a Drosophila synaptonemal complex protein. Genes Dev 15: 3130–3143.
45. Gloor GB, Preston CR, Johnson-Schlitz DM, Nassif NA, Phillis RW, et al. (1993) Type I Repressors of P Element Mobility. Genetics 135: 81–95.
46. Matthies HJ, Messina L, Namba R, Greer KJ, Walker MY, et al. (2000) Analysis of Meiosis in Fixed and Live Oocytes by Light Microscopy. In: Sullivan WS, Ashburner M, Hawley RS, eds. Drosophila: Protocols. New York: Cold Spring Harbor Press. pp 67–85.
47. Lantz V, Chang JS, Horabin JI, Bopp D, Schedl P (1994) The Drosophila orb RNA-binding protein is required for the formation of the egg chamber and establishment of polarity. Genes & Development 8: 598–613.
48. Anderson LK, Royer SM, Page SL, McKim KS, Lai A, et al. (2005) Juxtaposition of C(2)M and the transverse filament protein C(3)G within the central region of Drosophila synaptonemal complex. Proc Natl Acad Sci U S A 102: 4482–4487.
49. Liang L, Diehl-Jones W, Lasko P (1994) Localization of vasa protein to the Drosophila pole plasm is independent of its RNA-binding and helicase activities. Development 120: 1201–1211.
50. King RC, Rubinson AC, Smith RF (1956) Oogenesis in adult Drosophila melanogaster. Growth 20: 121–157.
51. Page SL, Khetani RS, Lake CM, Nielsen RJ, Jeffress JK, et al. (2008) Corona is required for higher-order assembly of transverse filaments into full-length synaptonemal complex in Drosophila oocytes. PLoS Genet 4: e1000194. doi:10.1371/journal.pgen.1000194.